Computer Physics Communications 36 (1985) 161–176
North-Holland, Amsterdam

TOPIC – A TOKAMAK PLASMA IMPURITIES CODE

T.A. BEU, F. SPINEANU, M. VLAD

Central Institute of Physics, Bucharest - Măgurele, Romania

R.I. CÂMPEANU

University of Cluj - Napoca, Department of Physics, 3400 Cluj - Napoca, Romania

and

I.I. POPESCU

University of Bucharest, Department of Physics, Bucharest - Măgurele, Romania

Received 20 August 1984

PROGRAM SUMMARY

Title of program: TOPIC

Catalogue number: ACDY

Program obtainable from: CPC Program Library, Queen's University of Belfast, N. Ireland (see application form in this issue)

Computer: CDC Cyber 170–720; *Installation*: Central Institute of Physics, Bucharest-Măgurele, Romania

Operating system: NOS1P4 552/552

Programming language used: FORTRAN IV

High speed storage required: 0.7 Kwords for the test run

No. of bits in a word: 60

Peripherals used: card reader, line printer, magnetic disk

No. of lines in combined program and test deck: 1217

Keywords: tokamak, plasma, impurities, diffusion equation, coupled differential equations, three-diagonal block matrix inversion

Nature of physical problem
In high temperature–low density tokamak plasmas, radiation cooling by impurity atoms can be an important energy loss mechanism [1,2], since radiation is not reabsorbed. The coupled set of time-dependent diffusion equations for ionized tokamak plasma impurities is solved in conjunction with a simple model for neutral impurities, on the assumption of a cylindrical symmetry. The resultant density distributions are used in the subsequent computation of the related energy losses.

Method of solution
The set of coupled second order differential equations, describing the diffusion of impurities in the MHD approach, is discretized using a finite difference scheme. The resultant linear system, with a three-diagonal block matrix structure, is then solved by a special forward elimination–backward substitution technique.

Typical running time
About 6 s for the test run output

References
[1] H.W. Drawin, Phys. Rep. 37 (1978) 125.
[2] H.W. Drawin, Phys. Scripta 24 (1981) 622.

LONG WRITE-UP

1. Introduction

The ideal magnetically confined fusion plasma would consist only of hydrogen isotopes, helium ions and the neutralizing electrons, well separated from the material walls of the reaction chamber by suitably shaped magnetic fields. In practice, high energy plasma particles leak across the magnetic field, strike the walls and liberate wall material, which diffuses into the plasma, where the impurity atoms (such as carbon, oxygen, iron, nickel, molybdenum) are ionized and excited. Ionization and excitation are accompanied by radiative decay and radiative and dielectronic recombination which lead to unwanted energy losses in addition to the bremsstrahlung radiation. These radiation losses lead to the cooling of the plasma [1,2].

2. Method of solution

The model adopted for the neutral impurities assumes that these flow into the plasma at thermal velocity V_0 and their density, $n_0(r)$, decreases rapidly through ionization as the impurities penetrate the plasma. Using the coordinates indicated in fig. 1 we have

$$n_0(r) = \frac{n_0^+}{4\pi} \int_0^{2\pi} d\varphi \int_{-\pi/2}^{\pi/2} d\psi \cos\psi \exp\left[-\frac{1}{V_0} \int_0^{\rho_s} \alpha_1(\rho') n_e(\rho')\, d\rho' \right], \tag{1}$$

where n_0^+ is the average number of neutrals leaving the material walls from the unit area. MKS units are used throughout the paper, except where specifically mentioned. In eq. (1) α_1 is the ionization rate for the neutrals and n_e is the electron density. V_0 is approximately given by the following expression

$$V_0 = 4 \times 10^{-10} (T_0/m_z)^{1/2},$$

where T_0 is the temperature of the neutrals (in eV) and m_z is the mass of the impurity.

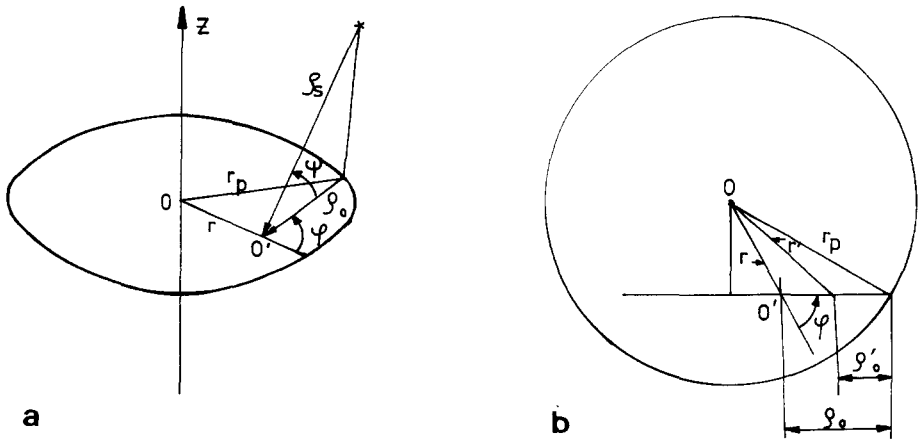

Fig. 1. Coordinates employed in the model for neutral impurities.

Taking into account the symmetric contributions, the integral (1) can be expressed as

$$n_0(r) = \frac{n_0^+}{\pi} \int_0^{\pi} \mathrm{d}\varphi \, \mathrm{Ki}_2\left[-\frac{1}{V_0} \int_0^{\rho_0} \alpha_1(\rho_0') n_e(\rho_0') \, \mathrm{d}\rho_0' \right], \tag{2}$$

where Ki_2 is the Bickley function of the second kind [3], defined as

$$\mathrm{Ki}_2(x) = \int_0^{\pi/2} \mathrm{d}\psi \cos\psi \exp(-x/\cos\psi). \tag{3}$$

In order to evaluate $n_0(r)$ one needs 2 further relations:

$$\rho_0 = \left(r_p^2 - r^2 \sin^2\varphi\right)^{1/2} - r\cos\varphi, \tag{4}$$

$$r' = \left((\rho_0 - \rho_0' + r\cos\varphi)^2 + r^2 \sin^2\varphi\right)^{1/2}, \tag{5}$$

where r' represents the position of the integration point with respect to the z axis, corresponding to the argument ρ_0'.

The density distributions of the ionized impurities are calculated by taking into account classical and anomalous diffusion and the ionization–recombination process. The radial density distributions are then given by the following set of coupled differential equations:

$$\frac{\partial n_k}{\partial t} + \frac{1}{r}\frac{\partial}{\partial r}(r\Phi_k) - n_e\left[(1-\delta_{k,1})\alpha_k n_{k-1} - (\alpha_{k+1} + \beta_k) n_k + \beta_{k+1} n_{k+1}\right] = \delta_{k,1} n_e \alpha_1 n_0,$$
$$k = 1, 2, \ldots, \mathrm{NST}, \tag{6}$$

where n_k is the impurity ion density in the kth ionization state, α_k is the ionization rate for the passage from the $(k-1)$th state to the kth state and β_k is the total recombination rate for the passage from the kth state to the $(k-1)$th state. NST represents the total number of ionization states and δ is Kronecker's symbol.

The flux of the impurity ions in the kth ionization state is given [4,5] as

$$\Phi_k = -\gamma_D D_k \partial n_k/\partial r + \gamma_W W_k n_k, \tag{7}$$

on the assumption that the impurity ion density is low enough for the effect of mutual collisions to be neglected. The Pfirsch–Schlüter diffusion coefficient D_k and the inward diffusion velocity due to friction with plasma ions W_k are, respectively, given by

$$D_k = (1+q^2)\rho_k^2 \nu_k, \tag{8}$$

$$W_k = k D_k \left(\frac{1}{n_i}\frac{\mathrm{d}n_i}{\mathrm{d}r} - \frac{1}{2T_i}\frac{\mathrm{d}T_i}{\mathrm{d}r}\right), \tag{9}$$

where γ_D and γ_W are the anomaly factors. The safety factor q, the squared Larmor radius ρ_k^2, and the collision frequency of impurity ions with plasma ions ν_k, are defined as follows:

$$q = \frac{r}{R_t}\frac{B_t}{B_p}, \tag{10}$$

$$\rho_k^2 = 6.25 \times 10^{18} \frac{m_z}{B_t^2}\frac{T_k}{k^2}, \tag{11}$$

$$\nu_k = 2.765 \times 10^{-27} n_i (m_i)^{1/2} k^2 \ln \Lambda_k / \left(m_z T_i^{3/2}\right). \tag{12}$$

Here R_t is the major radius of the reaction chamber, B_t and B_p are the toroidal and the poloidal magnetic fields, respectively, n_i is the plasma ion density,

$$\ln \Lambda_k = \ln\left[1.552 \times 10^{13} \frac{T_i^{3/2}}{(\bar{Z} n_e)^{1/2}} \frac{1}{k}\right] \tag{13}$$

is the Coulomb logarithm, T_i is the plasma ion temperature and T_k is the impurity ion temperature (in eV). The effective ionic charge of the plasma, $\bar{Z}$, is defined as

$$\bar{Z} = \left(n_i + \sum_{k=1}^{NST} k^2 n_k\right)/n_e \tag{14}$$

and according to charge neutrality

$$n_i = n_e - \sum_{k=1}^{NST} k n_k. \tag{15}$$

The diffusion coefficients depend on the impurity ion temperature T_k, for which we used the following simple model:

$$T_k = \begin{cases} \text{given constant} & (k=0), \\ T_i \text{ for } \tau_{eq} \leqslant \tau_i & (k \neq 0), \\ \min\left[T_i,\ T_{k-1} + (T_i - T_{k-1})\tau_i/\tau_{eq}\right] \text{ for } \tau_{eq} > \tau_i & (k \neq 0), \end{cases} \tag{16}$$

where

$$\tau_i = 1/(\alpha_{k+1} + \beta_k) n_e \tag{17}$$

and

$$\tau_{eq} = 1/2\nu_k. \tag{18}$$

This program uses the ionization rates α_k given by the formula of Lotz [6]

$$\alpha_k = 67 \sum_{i=1}^{NSS} \frac{a_i^k q_i^k}{T_e^{3/2}} \left[\frac{1}{P_i^k/T_e} E_1\left(\frac{P_i^k}{T_e}\right) - \frac{b_i^k \exp(c_i^k)}{P_i^k/T_e + c_i^k} E_1\left(\frac{P_i^k}{T_e} + c_i^k\right)\right], \tag{19}$$

where

$$E_1(x) = \int_x^\infty [\exp(-y)/y]\, dy$$

is the exponential integral, P_i^k is the binding energy of the electrons in the ith subshell (in eV), q_i^k is the number of equivalent electrons in this subshell and a_i^k, b_i^k and c_i^k are fitting constants tabulated in ref. [6]. NSS stands for the number of subshells considered. The ionization rates of Lotz were found quite satisfactory, especially for light atoms where autoionization is less important.

Taking into account the radiative recombination rate β_k^r [8] and the dielectronic recombination rate β_k^d [9], the approximate expression for the total recombination rate is $\beta_k = \beta_k^r + \beta_k^d$, with

$$\beta_k^r = 2.6 \times 10^{-20} k^2 \left\{\left(\frac{P_H}{T_e}\right)^{1/2} \frac{\xi P_1^k}{n^3 T_e} E_1'\left(\frac{P_1^k}{T_e}\right) + 2k^2 \left(\frac{P_H}{T_e}\right)^{3/2} \sum_{i=1}^{\infty} \frac{1}{(n+i)^3} E_1'\left[\frac{k^2 P_H}{(n+i)^3 T_e}\right]\right\}, \tag{20}$$

where

$$E_1'(x) = \exp(x) E_1(x). \tag{21}$$

In (20) n is the principal quantum number of the ground state, ξ is the number of empty places in the valence shell, P_H is the ionization potential of hydrogen.

For impurities with NST $\leqslant 21$ we use

$$\beta_k^d = 10^{-16} A(k) \left[\frac{E_T(k,1)}{T_e}\right]^{3/2} \exp\left[-\frac{E_T(k,1)}{T_e}\right] \tag{22}$$

with $A(k)$ a coefficient depending on the type of transition and with $E_T(k, 1)$ representing the energy of the first resonant transition of the ion. For NST > 21 we use

$$\beta_k^d = 2.4 \times 10^{-15} \frac{A(k)}{T_e^{3/2}} \sum_{j=1}^{2} f_{kj} B(k, j) \exp[-C(k, j)/T_e], \tag{22'}$$

where $k_1 = k + 1$,

$$A(k) = \left[\frac{k_1(k_1+1)}{(k_1^2+13.4)}\right]^{1/2}, \quad x_{kj} = \frac{E_T(k, j)}{(k_1+1)P_H},$$

$$B(k, j) = \frac{x_{kj}}{1 + 0.105x_{kj} + 0.015x_{kj}^2}, \quad C(k, j) = \frac{1.36(k_1+1)x_{kj}}{1 + 0.015k_1^3/(k_1+1)^2},$$

and where f_{kj} represents the oscillator strength.

Eqs. (6) are solved under the following boundary conditions:

$$\begin{aligned} &[n_0(r)]_{r=r_p} = \text{given constant}, \\ &[n_k(r)]_{r=r_p} = 0, \quad k = 1, 2, \ldots, \text{NST}, \\ &\left[\frac{\partial n_k}{\partial r}\right]_{r=0} = 0, \quad k = 1, 2, \ldots, \text{NST}, \end{aligned} \tag{23}$$

and in considering the time-dependent cases one adds the initial conditions

$$n_k^{t=0}(r) = n_k^0(r), \quad k = 1, 2, \ldots, \text{NST}. \tag{24}$$

The energy losses by ionization, recombination, bremsstrahlung and excitation due to the presence of impurities are approximately given by

$$\begin{aligned} p_i &= 1.6 \times 10^{-19} \sum_{k=1}^{\text{NST}} n_e n_{k-1} \alpha_k \left(P_1^k + \tfrac{3}{2} T_e\right) + p_{rec}, \\ p_{rec} &= 1.6 \times 10^{-19} \sum_{k=1}^{\text{NST}} \left(\tfrac{3}{2} n_e n_k \beta_k T_e\right), \\ p_{br} &= 1.5 \times 10^{-38} \bar{Z} n_e^2 T_e^{1/2}, \\ p_{ex} &= 1.73 \times 10^{-31} T_e^{-1/2} n_e \sum_{k=1}^{\text{NST}-1} n_k \sum_{l=1}^{L} c_{kl} \exp\left(-\frac{P_{ex}}{T_e}\right), \end{aligned} \tag{25}$$

where P_{ex} is the excitation potential. The coefficients c_{kl} are tabulated in ref. [5].

3. Numerical aspects

Both the stationary and the time-dependent impurity transport problem are considered. Let us discuss first the stationary case, that is eq. (6) with vanishing time derivative of the particle flux. The equations were approximated by simple finite difference schemes:

$$\frac{1}{r^m}\left\{\frac{-2}{h^m+h^{m-1}}\left[\frac{r^m D_k^m + r^{m-1}D_k^{m-1}}{2}\,\frac{n_k^m - n_k^{m-1}}{h^{m-1}} - \frac{r^{m+1}D_k^{m+1} + r^m D_k^m}{2}\,\frac{n^{m+1}-n_k^m}{h^m}\right]\right.$$
$$\left. - \frac{1}{2r^m}\left[\frac{r^m W_k^m n_k^m - r^{m-1}W_k^{m-1}n_k^{m-1}}{h^{m-1}} + \frac{r^{m+1}W_k^{m+1}n_k^{m+1} - r^m W_k^m n_k^m}{h^m}\right]\right\}$$
$$- n_e^m\left[(1-\delta_{k,1})\alpha_k^m n_{k-1}^m - (\alpha_{k+1}^m + \beta_k^m)n_k^m + \beta_{k+1}^m n_{k+1}^m\right] = \delta_{k,1} n_e^m \alpha_1^m n_0^m,$$
$$k = 1, 2, \ldots, \mathrm{NST},\ m = 2,3,\ldots,\mathrm{NMP}-1, \tag{26}$$

where m denotes the mesh point, $h^{m-1} = r^m - r^{m-1}$, $h^m = r^{m+1} - r^m$ and NMP represents the number of mesh points. This linear system can be finally written as

$$\sum_{k=1}^{\mathrm{NST}}\left[A_{jk}^m n_k^{m-1} + B_{jk}^m n_k^m + C_{jk}^m n_k^{m+1}\right] = T_j^m, \qquad j = 1, 2, \ldots, \mathrm{NST},\ m = 2,3,\ldots,\mathrm{NMP}-1, \tag{27}$$

with

$$A_{jk}^m = \left(-d_j^{m1} - \frac{1}{2h^{m-1}}\frac{r^{m-1}}{r^m}W_j^{m-1}\right)\delta_{jk},$$

$$B_{jk}^m = \begin{cases} -(1-\delta_{k,1})n_e^m\alpha_j^m, & k = j-1, \\ d_j^{m1} + d_j^{m2} + \frac{1}{2}\left(\frac{1}{h^{m-1}} - \frac{1}{h^m}\right)W_j^m + n_e^m(\alpha_{j+1}^m + \beta_j^m), & k = j, \\ -n_e\beta_{j+1}^m, & k = j+1, \\ 0, & k \neq j,\ k \neq j \pm 1, \end{cases} \tag{28}$$

$$C_{jk}^m = \left(-d_j^{m2} + \frac{1}{2h^m}\frac{r^{m+1}}{r^m}W_j^{m+1}\right)\delta_{jk},$$
$$T_j^m = \delta_{k,1} n_e^m \alpha_1^m n_0^m,$$

where

$$d_j^{m1} = \frac{(r^{m-1}/r^m)D_j^{m-1} + D_j^m}{(h^{m-1}+h^m)h^{m-1}}, \qquad d_j^{m2} = \frac{(r^{m+1}/r^m)D_j^{m+1} + D_j^m}{(h^{m-1}+h^m)h^m}. \tag{29}$$

The use of the Crank–Nicholson scheme for the time-dependent transport equation yields a linear system similar to the one obtained for the stationary case:

$$\sum_{k=1}^{\mathrm{NST}}\left[A_{jk}^{m,t} n_k^{m-1,t} + B_{jk}^{m,t} n_k^{m,t} + C_{jk}^{m,t} n_k^{m+1,t}\right] = T_j^{m,t}, \tag{30}$$

with

$$A_{jk}^{m,t} = A_{jk}^{m}, \quad B_{jk}^{m,t} = B_{jk}^{m} + (2/h_t)\delta_{jk}, \quad C_{jk}^{m,t} = C_{jk}^{m}, \tag{31}$$

$$T_j^{m,t} = 2T_j^m - A_{jj}^m n_j^{m-1,t'} - B_{j,j-1}^m n_{j-1}^{m,t'} - \left(B_{jj}^{m,t} - \frac{2}{h_t}\right) n_j^{m,t'} - B_{j,j+1}^{m,t} n_{j+1}^{m,t'} - C_{jj}^m n_j^{m+1,t'}, \quad t' = t + h_t.$$

Taking into account the three-diagonal block structure of the discretized linear system matrix, a special forward elimination–backward substitution technique was used to solve this system. The method is equivalent to supposing a linear dependence between the densities in two neighbouring mesh points:

$$n_j^m = F_j^m - \sum_{k=1}^{\mathrm{NST}} G_{jk}^m n_k^{m+1}. \tag{32}$$

This linear dependence represents in fact the recurrence relation of the backward substitution sweep. The recurrence relations for the forward elimination sweep may be derived by substituting eq. (32) into eq. (27) (or into eq. (30) for the time-dependent case) for both n_k^{m+1} and n_k^m. One thus obtains the following equations (by denoting by G'^m_{jk} the elements of the matrix obtained by the inversion of the matrix having the elements G_{jk}^m):

$$G'^m_{jk} = \left(B_{jk}^m - A_{jj}^m G_{jk}^{m-1}\right)/C_{jj}^m, \tag{33}$$

$$\sum_{k=1}^{\mathrm{NST}} G'^m_{jk} F_k^m = \left(T_j^m - A_{jj}^m F_j^{m-1}\right)/C_{jj}^m. \tag{34}$$

From the boundary conditions (23) n_k can be expressed approximately as

$$n_k^1 = \tfrac{4}{3} n_k^2 - \tfrac{1}{3} n_k^3. \tag{35}$$

This supplementary relation allows us to obtain independent relations for F_j^2 and G_{jk}^2:

$$G_{jk}^2 = \left(B_{jk}^2 + \tfrac{4}{3} A_{jj}^2 \delta_{jk}\right)/\left(C_{jj}^2 - \tfrac{1}{3} A_{jj}^2\right), \tag{36}$$

$$\sum_{k=1}^{\mathrm{NST}} G'^2_{jk} F_k^2 = T_j^2/\left(C_{jj}^2 - \tfrac{1}{3} A_{jj}^2\right), \tag{37}$$

The solution of the discretized stationary system (27) can be iterated according to charge neutrality (15). This non-linear iteration scheme, consisting of NNI iterations, is due to the fact that the stationary algorithm must be provided with an initial guess for $\overline{Z}$ and n_i.

The computation of the exponential integral (eqs. 5.1.53 and 5.1.56 in ref. [10]) and of the Bickley function [3] was accomplished with polynomial and rational approximations, for which the errors are less than 2×10^{-7}.

4. Code description

TOPIC consists of a main program, 20 subroutine-type subprograms and 3 function-type subprograms, structured as in the block-diagram shown in fig. 2.

Subroutine START reads necessary data (NST, NSS, NMP) for the subsequent computation of the number of words required by the arrays used in the program:

NW = NST * (24 + 3 * NST + NMP) + 12 * (NMP + NSS)

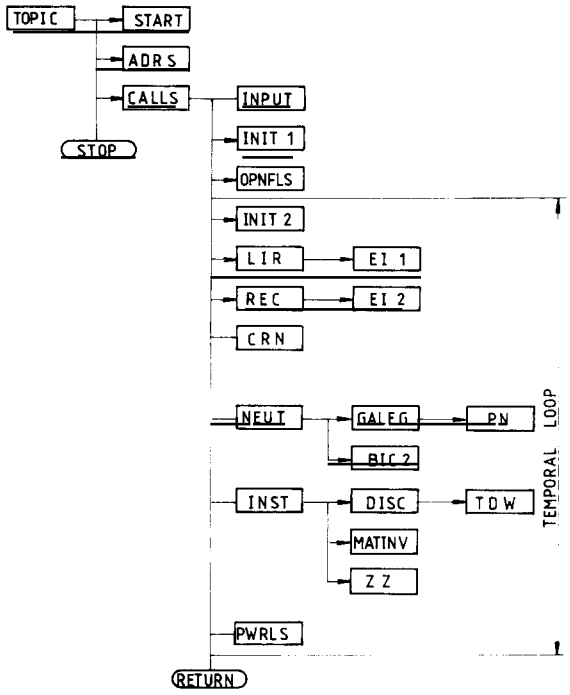

Fig. 2. Flow diagram of TOPIC.

On return to the main program, NW is used by the system subprograms SYMLIB, CMMALF and LOCF for dynamic memory allocation, relative to the starting address of the array A dimensioned in the main program. On computers which do not have dynamic memory allocation facilities the sequence

```
CALL SYMLIB
CALL CMMALF(NW + 1, 0, 0, IA)
LA = IA - LOCF(A(1)) + 1
```

should be replaced by

```
LA = 1
```

while the array A should be dimensioned according to NW. Subroutine START also prints the heading of the program and the current date by calling the system subroutine DATE.

Subroutine ADRS computes starting addresses for the arrays used by the program relative to the "new" starting address of the array A, that is LA.

Subroutine CALLS has two purposes. First, it makes the correspondence between the starting addresses of the arrays of the program and the addresses of the appropriate components of the vector A. Second, it calls the subprograms of the next level (see flow-chart) which benefit of a simple variable dimensioning.

Subroutine INPUT reads most of the input data:

AD	coefficient for dielectronic recombination [$A(k)$ in eqs. (22), (22′)],
AL, BL, CL	coefficients for ionization rates [a_i^k, b_i^k, c_i^k in eq. (19)],
CPW	coefficient for excitation energy losses [c_{kl} in eq. (25)],
ET	transition energy for dielectronic recombination [E_T in eq. (22)],
FF	oscillator strength [f_{kj} in eq. (22′)],

HIEX	excitation potential [P_{ex} in eq. (19)],
PL	binding energy for electrons [P_i^k in eq. (19)],
LQ	number of equivalent electrons in a subshell [q_i^k in eq. (19)],
NLL	number of empty places in the valence shell [ξ in eq. (20)],
NPF	principal quantum number of the ground state [n in eq. (20)],
GAMAD, GAMAW	anomaly factors for diffusion coefficients [γ_D, γ_W in eq. (7)],
HD	hydrogen/(hydrogen + deuterium) ratio of the plasma; for HD = 1 plasma contains only hydrogen, while for HD = 0 plasma consists only of deuterium,
HT	temporal step size,
MZ	impurity ion mass,
NGP	number of Gaussian integration points for the computation of the neutral densities,
RP	poloidal radius,
RT	toroidal radius,
TO	temperature of neutrals,
NNI	number of nonlinear iterations,
NTI	number of temporal iterations,
IOPTN	normalization option variable for impurity densities,
INPRR, INPBP, INPTE, INPTI	input options for mesh, poloidal magnetic field, electron density, electron temperature and plasma ion temperature, respectively.

All the input data is printed in an explicit manner.

Subroutine INIT1 reads for INPRR = 1 the values of the poloidal mesh point distances to the axis of the plasma column. For INPRR = 0 the code initializes a mesh having equidistant points. Subroutine INIT1 also zeroes the impurity density.

Subroutine OPNFLS opens the mass storage random access files on which ionization rates, recombination rates and the arrays G and F (used for the iterative solution of the discretized system) are stored.

Subroutine INIT2 is called at each temporal step (once for the stationary case). According to the values of the variables INPBP, INPNE, INPTE, INPTI, the values for the corresponding profiles are read(option 1), or initialized by reading only a few input data(option 0). If INPBP = 0 the poloidal magnetic field is initialized as

$$B_p(r) = 2\times 10^{-7} I_p / r\left\{1-\left[1-(r/r_p)^2\right]^2\right\}, \tag{38}$$

where I_p, the total plasma current, is input data (variable CTOT). If INPNE = 0 the electron density is initialized to a parabolic profile:

$$n_e(r) = n_e(0) + \left[n_e(r_p) - n_e(0)\right](r/r_p)^2, \tag{39}$$

where $n_e(0)$ and $n_e(r_p)$ are input data (variable NE(1) and NE(NMP)). The plasma ion density (variable NI) is taken equal to the electron density for the first temporal iteration, or in the stationary case. The electron temperature and plasma ion temperature profiles are initialized for INPTE = 0 and INPTI, respectively, by a three-order polynomial form:

$$T_e(r) = \left[2\left\{T_e(0) - T_e(r_p)\right\} + \mathrm{STE}\right](r/r_p)^3 - \left[3\left\{T_e(0) - T_e(r_p)\right\} + \mathrm{STE}\right](r/r_p)^2 + T_e(0), \tag{40}$$

$$T_i(r) = \left[2\left\{T_i(0) - T_i(r_p)\right\} + \mathrm{STI}\right](r/r_p)^3 - \left[3\left\{T_i(0) - T_i(r_p)\right\} + \mathrm{STI}\right](r/r_p)^2 + T_i(0), \tag{41}$$

where STE and STI are the derivatives of the respective profiles at $r = r_p$. $T_e(0)$, $T_e(r_p)$, STE, $T_i(0)$, $T_i(r_p)$, STI are input data.

Subroutine LIR computes the ionization rates of Lotz [6] (vector ALFA in the program). It calls function EI1 which computes the exponential integral $E_1(x)$. The rates are stored for each mesh point on magnetic disk.

Subroutine REC computes total recombination rates (vector BETA). It calls function EI2 which computes $\exp(x)E_1(x)$ and stores the recombination rates on magnetic disk for each mesh point.

Subroutine CRN is called only for the stationary case. It computes impurity densities in the corona model [1,2], using the relations

$$\begin{aligned} n_0^m &= 1, \qquad m = 1,2,\ldots,\mathrm{NMP}, \\ n_k^m &= \frac{\alpha_k}{\beta_k} n_{k-1}^m, \quad k = 1,2,\ldots,\mathrm{NST}. \end{aligned} \tag{42}$$

These profiles will represent through the effective ionic charge, computed in subroutine ZZ, an initial guess for the diffusion model computation of the densities.

Subroutine ZZ normalizes the impurity density profiles according to the value of IOPTN. For IOPTN = 0 the profiles are normalized such that the total impurity density (neutrals plus ions) should represent at $r = 0$ the fraction CONC from the electron density at $r = 0$. For IOPTN = 1 the same procedure is applied at the point at which the total impurity density has the greatest value. For IOPTN > 1, CONC represents the ratio of the total impurity density space integral to the electron density space

Table 1
Description of the input data cards

No.	Input variables	Format	Observations
1	NST, NSS, NMP	24I3	
2	NGP, NNI, NTI, IOPTN, INPRR, INPBP, INPNE, INPTE, INPTI	24I3	
3	RP, BT, RT, GAMAD, GAMAW, HD	8F9.4	
4	TO, MZ, CONC	3E12.4	
5	((LQ(I, J), I = 1, NST), J = 1, NSS)	24I3	
6	((PL(I, J), I = 1, NST), J = 1, NSS)	8F9.4	
7	((AL(I, J), I = 1, NST), J = 1, NSS)	8F9.4	
8	((BL(I, J), I = 1, NST), J = 1, NSS)	8F9.4	
9	((CL(I, J), I = 1, NST), J = 1, NSS)	8F9.4	
10	((ET(I, J), I = 1, NST), J = 1, 2)	8F9.4	
11	(AD(I), I = 1, NST)	8F9.4	
12	((FF(I, J), I = 1, NST), J = 1, 2)	8F9.4	
13	((CPW(I, J), J = 1, NST1), I = 1, NST1)	7F9.4	
14	(HIEX(I, J), J = 1, NST1), I = 1, NST1)	7F9.4	
15	(NPF(I), I = 1, NST)	24I3	
16	(NLL(I), I = 1, NST)	24I3	
17	HT	3E12.4	IF(NTI.NE.0)
18	(R(M), M = 1, NMP)	3E12.4	IF(INPRR.EQ.1)
19	CTOT	3E12.4	IF(INPBP.EQ.0)
20	(BP(M), M = 1, NMP)	3E12.4	IF(INPBR.EQ.1)
21	NE(1), NE(NMP)	3E12.4	IF(INPNE.EQ.0)
22	(NE(M), M = 1, NMP)	3E12.4	IF(INPNE.EQ.1)
23	TE(1), TE(NMP), STE	3E12.4	IF(INPTE.EQ.0)
24	(TE(M), M = 1, NMP)	3E12.4	IF(INPTE.EQ.1)
25	TI(1), TI (NMP), STI	3E12.4	IF(INPTI.EQ.0)
26	(TI(M), M = 1, NMP)	3E12.4	IF(INPTI.EQ.1)

integral. The option IOPTN = 1 was found to give always correct results, while the other options can yield errors when the impurity densities and temperatures reach high values.

Subroutine NEUT computes neutral densities according to eq. (2). It calls subroutine GALEG to generate Gaussian integration points. About 4 integration points are found sufficient in most cases. Subroutine NEUT also calls function BIC2 for the computation of the Bickley function.

SUBROUTINE INST computes densities for the ionized states of the impurity by using the algorithm (32)–(37). It calls subroutine DISC, which computes the discretization coefficients A^m_{jk}, B^m_{jk}, C^m_{jk} and T^m_j employed in the stationary equation (27) or in the time-dependent equation (30). DISC calls subroutine TDW which computes impurities temperatures and diffusion coefficients (D_k and W_k). Subroutine INST also calls subroutines MATINV and ZZ. MATINV solves the matrix equation AX = B, replacing A by A^{-1} and B by X. INST allows for NNI nonlinear iterations according to charge neutrality (15).

5. Input

The description of the input data cards is given in table 1. Each line in the table corresponds to a data card, except in the cases when the variables correspond to arrays of dimensions given by NSS, NST, NST1 = NST − 1 and NMP. The lines 19–26 are read at each temporal step, while in the stationary case they are read only once.

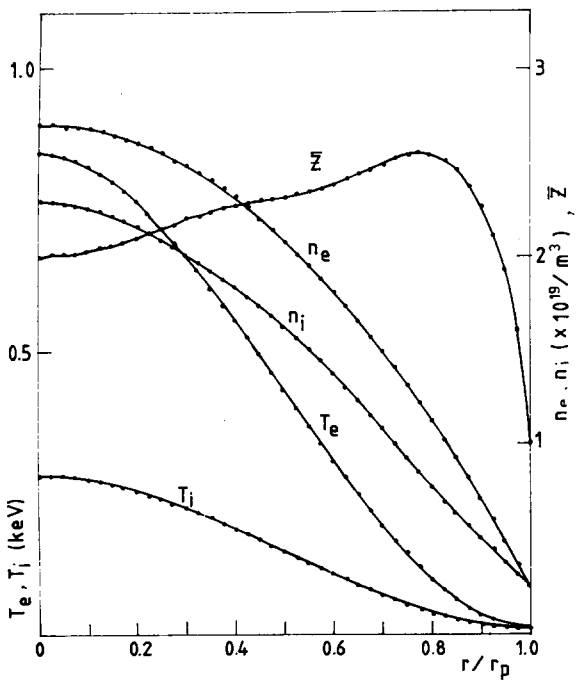

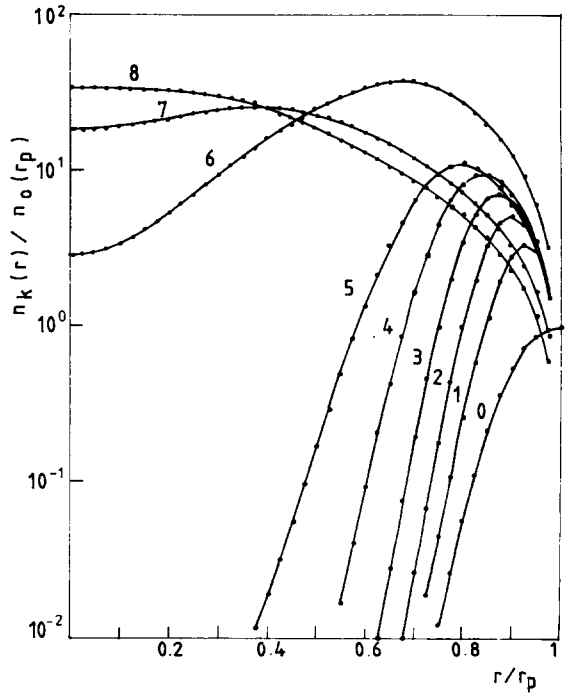

Fig. 3. Input profiles for n_e, T_e, T_i and the output profiles for n_i and $\bar{Z}$ calculated by TOPIC.

Fig. 4. The impurity density profiles given numerically in the test run output.

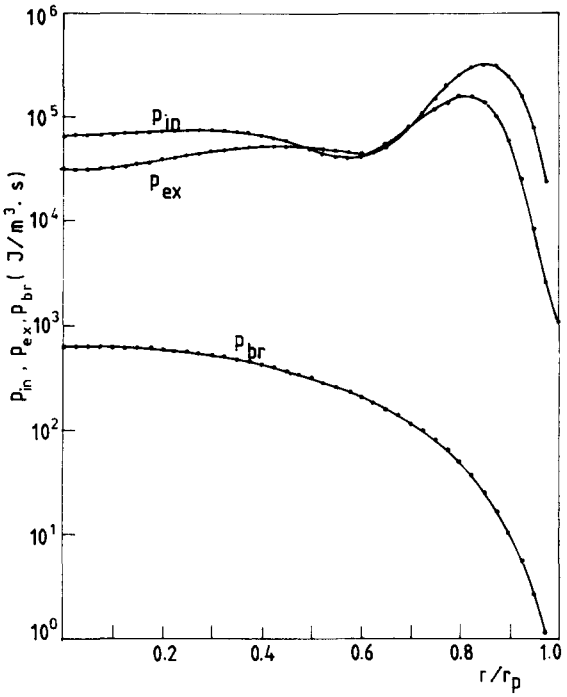

Fig. 5. Radiative energy losses obtained with the impurity density profiles of fig. 4.

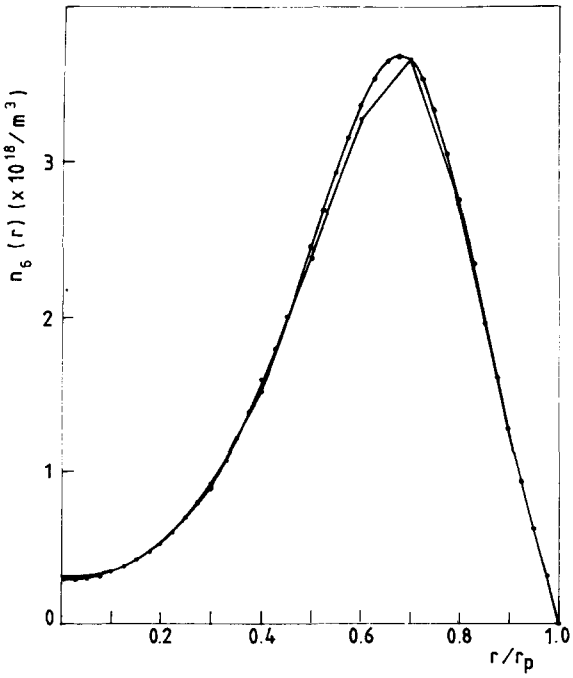

Fig. 6. The variation of $n_6(r)$ obtained with 11 (lower curve) and 41 mesh points respectively.

6. Test run

The code was tested for oxygen impurity ions with the input data similar, but not exactly the same, as in ref. [5]. The test run deck consists of two cases: a stationary and a time-dependent one. The test run output presents the results only for the stationary problem. These results, which can be compared with those of ref. [5] are discussed in what follows.

Fig. 3 presents our input profiles for the electron density n_e, electron temperature T_e, plasma ion temperature T_i and the output profiles for plasma ion density and for effective ionic charge $\bar{Z}$. The input profiles are generated by the coded polynomial approximations (39)–(41).

Fig. 4 shows the resulting impurity density profiles. The figures attached to each curve denote the ionization state of the impurity (the neutrals are labelled with 0, the simple ionized oxygen with 1, etc.). Our results are seen to agree qualitatively with those of Tazima et al. [5]. Fig. 5 gives the radiative energy losses obtained with the impurity density profiles of fig. 4.

7. Accuracy test

We have tested the influence of the spatial mesh grid upon the accuracy of the impurity density values. Fig. 6 compares the profiles obtained for O^{6+} by using 11 and 41 mesh points, respectively. The differences between the two profiles appear to be very small, with a maximum of 2.5%.

References

[1] H.W. Drawin, Phys. Rep. 37 (1978) 125.
[2] H.W. Drawin, Phys. Scripta 24 (1981) 622.
[3] W.G. Bickley and J. Nayler, Phil. Mag. 20 (1935) 343.
[4] A. Samain, EUR-CEA-FC-745 (1974).
[5] T. Tazima, Y. Nakamura and K. Inoue, Nucl. Fusion 17 (1977) 419.
[6] W. Lotz, IPP 1/62 (1967).
[7] K.L. Bell, H.B. Gilbody, J.G. Hughes, A.E. Kingston and F.J. Smith, Report CLM-R216 (1982).
[8] S. von Goeler, W. Stodiek, H. Eubank, H. Fishman, S. Grebenshchikov and E. Hinnov, Nucl. Fusion 15 (1975) 301.
[9] EUR-CEA, MAKOKOT – Code d'evolution (August 1977).
[10] M.Abramowitz and I.A. Stegun, Handbook of Mathematical Functions (Dover, New York, 1970).

TEST RUN OUTPUT

Input data

```
WORDS OF CORE REQUIRED                                  634

EXCEPT WHERE SPECIFIED DATA ARE IN MKS UNITS

DATA ON INSTALLATION ##########################
RT      TOROIDAL RADIUS                                  1.09000
RP      POLOIDAL RADIUS                                   .12000
BT      POLOIDAL MAGNETIC FIELD                          2.70000
DATA ON PLASMA ################################
HD      HIDR.TO (HIDR.+DEUT.) FRACTION                   1.00000
DATA ON IMPURITY ##############################
MZ      ION MASS                                     .26560E-25
NST     NO.OF IONIZED STATES                                  8
NSS     NO.OF SUBSHELLS                                       2
TO      TEMPERATURE OF NEUTRALS  (EV)                .50000E+01
CCNC    CONCENTRATION                                .30000E-01
IOPTN   NORMALIZATION OPTION                                  1
GAMAD   PFIRSCH-SCHLUTER ANOMALITY FACTOR                1.00000
GAMAW   INWARD DIFF.VELOCITY ANOMALITY FACTOR            1.00000
NUMERICAL DATA ################################
NMP     NO. OF MESH POINTS                                   11
NGP     NO. OF GAUSSIAN INTEGRATION POINTS                    4
NNI     NO. OF NONLINEAR ITERATIONS                           3
NTI     NO. OF TEMPORAL ITERATIONS                            0
```

MESH POINT	POLOIDAL MAG.FIELD	PLASMA TEMPERATURES ELECTRONS	TEMPERATURES IONS	ELECTRON DENSITY
1	.133E-01	.850E+03	.280E+03	.270E+20
2	.133E-01	.826E+03	.272E+03	.268E+20
3	.261E-01	.763E+03	.252E+03	.260E+20
4	.382E-01	.669E+03	.222E+03	.248E+20
5	.491E-01	.554E+03	.185E+03	.231E+20
6	.583E-01	.430E+03	.145E+03	.209E+20
7	.656E-01	.306E+03	.105E+03	.182E+20
8	.705E-01	.191E+03	.683E+02	.150E+20
9	.728E-01	.974E+02	.361E+02	.113E+20
10	.714E-01	.333E+02	.176E+02	.716E+19
11	.667E-01	.100E+02	.100E+02	.250E+19

Output data

```
CORONA MODEL###
```

MESH POINT	NEUTRAL DENSITIES	EFFECTIVE CHARGE
1	.206E+20	.264E+01
2	.222E+20	.218E+01
3	.243E+20	.145E+01
4	.245E+20	.109E+01
5	.230E+20	.101E+01
6	.209E+20	.100E+01
7	.182E+20	.100E+01
8	.150E+20	.100E+01
9	.113E+20	.100E+01
10	.716E+19	.100E+01
11	.250E+19	.100E+01

MESH POINT — NEUTRAL AND ION DENSITIES (INCREASING CHARGE)

1	.123E-14	.837E-06	.207E+00	.977E+04	.117E+09	.451E+12	.217E+16	.679E+17	.740E+18
2	.123E-14	.812E-06	.193E+00	.877E+04	.101E+09	.371E+12	.171E+16	.508E+17	.524E+18
3	.123E-14	.743E-06	.158E+00	.641E+04	.653E+08	.213E+12	.862E+15	.220E+17	.193E+18
4	.123E-14	.643E-06	.114E+00	.381E+04	.319E+08	.843E+11	.276E+15	.546E+16	.364E+17
5	.123E-14	.521E-06	.710E-01	.180E+04	.113E+08	.220E+11	.528E+14	.716E+15	.318E+16
6	.123E-14	.390E-06	.368E-01	.636E+03	.268E+07	.339E+10	.521E+13	.412E+14	.101E+15
7	.123E-14	.262E-06	.148E-01	.149E+03	.356E+06	.244E+09	.199E+12	.705E+12	.682E+12
8	.123E-14	.147E-06	.394E-02	.179E+02	.184E+05	.502E+07	.154E+10	.144E+10	.258E+09
9	.123E-14	.987E-07	.472E-03	.581E+00	.146E+03	.813E+04	.440E+06	.132E+05	.236E+02
10	.123E-14	.988E-08	.757E-05	.638E-03	.727E-02	.987E-02	.706E-02	.378E-10	.820E-21
11	.123E-14	.554E-09	.824E-08	.405E-08	.583E-10	.110E-13	.114E-18	.429E-50	.637E-88

```
***DIFFUSION MODEL***

NON LINEAR ITERATION NO.    1
     MESH NEUTRAL   EFFECTIVE
    POINT DENSITIES CHARGE
        1  .268E+20  .106E+01
        2  .264E+20  .109E+01
        3  .252E+20  .120E+01
        4  .235E+20  .131E+01
        5  .215E+20  .14CE+01
        6  .191E+20  .148E+01
        7  .163E+20  .158E+01
        8  .130E+20  .170E+01
        9  .947E+19  .178E+01
       10  .596E+19  .17CE+01
       11  .850E+19  .100E+01
     MESH NEUTRAL AND ION DENSITIES
    POINT (INCREASING CHARGE)
        1  .790E+00  .588E+02  .246E+03  .915E+06  .113E+10  .218E+13  .348E+16  .157E+17  .131E+17
        2  .206E+02  .588E+02  .246E+03  .915E+06  .113E+10  .218E+13  .808E+16  .252E+17  .195E+17
        3  .273E+04  .794E+04  .451E+05  .507E+06  .176E+11  .898E+13  .219E+17  .538E+17  .387E+17
        4  .356E+06  .105E+07  .821E+07  .243E+10  .350E+12  .459E+14  .460E+17  .819E+17  .517E+17
        5  .384E+08  .118E+09  .127E+10  .105E+12  .668E+13  .300E+15  .812E+17  .944E+17  .504E+17
        6  .433E+10  .140E+11  .144E+12  .390E+13  .111E+15  .202E+16  .129E+18  .903E+17  .413E+17
        7  .328E+12  .115E+13  .908E+13  .113E+15  .143E+16  .110E+17  .180E+18  .749E+17  .314E+17
        8  .151E+14  .638E+14  .338E+15  .216E+16  .121E+17  .391E+17  .200E+18  .554E+17  .230E+17
        9  .361E+15  .176E+16  .643E+16  .204E+17  .468E+17  .625E+17  .150E+18  .360E+17  .150E+17
       10  .329E+16  .171E+17  .376E+17  .464E+17  .367E+17  .334E+17  .771E+17  .186E+17  .771E+16
       11  .743E+16 0.         0.         0.         0.         0.         0.         0.
NON LINEAR ITERATION NO.    2
     MESH NEUTRAL   EFFECTIVE
    POINT DENSITIES CHARGE
        1  .223E+20  .214E+01
        2  .221E+20  .215E+01
        3  .214E+20  .215E+01
        4  .203E+20  .216E+01
        5  .186E+20  .219E+01
        6  .166E+20  .223E+01
        7  .141E+20  .23CE+01
        8  .111E+20  .240E+01
        9  .792E+19  .247E+01
       10  .500E+19  .228E+01
       11  .250E+19  .100E+01
     MESH NEUTRAL AND ION DENSITIES
    POINT (INCREASING CHARGE)
        1  .125E+01  .933E+02  .421E+03  .170E+07  .425E+10  .768E+13  .391E+17  .217E+18  .368E+18
        2  .324E+02  .933E+02  .421E+03  .170E+07  .425E+10  .113E+14  .454E+17  .220E+18  .358E+18
        3  .431E+04  .125E+05  .601E+05  .591E+08  .268E+11  .222E+14  .643E+17  .232E+18  .327E+18
        4  .560E+06  .165E+07  .946E+07  .258E+10  .422E+12  .762E+14  .101E+18  .241E+18  .280E+18
        5  .604E+08  .185E+09  .140E+10  .113E+12  .794E+13  .434E+15  .162E+18  .239E+18  .224E+18
        6  .683E+10  .216E+11  .165E+12  .441E+13  .136E+15  .286E+16  .243E+18  .212E+18  .164E+18
        7  .517E+12  .176E+13  .214E+14  .137E+15  .187E+16  .161E+17  .324E+18  .165E+18  .118E+18
        8  .238E+14  .936E+14  .456E+15  .291E+16  .174E+17  .614E+17  .349E+18  .113E+18  .783E+17
        9  .569E+15  .266E+16  .965E+16  .321E+17  .787E+17  .110E+18  .258E+18  .691E+17  .478E+17
       10  .518E+16  .277E+17  .646E+17  .858E+17  .662E+17  .571E+17  .127E+18  .342E+17  .235E+17
       11  .117E+17 0.         0.         0.         0.         0.         0.         0.
```

```
NON LINEAR ITERATION NO.    3
     MESH NEUTRAL   EFFECTIVE
    POINT DENSITIES CHARGE
        1  .230E+20  .199E+01
        2  .227E+20  .201E+01
        3  .218E+20  .206E+01
        4  .204E+20  .213E+01
        5  .186E+20  .220E+01
        6  .165E+20  .229E+01
        7  .140E+20  .231E+01
        8  .111E+20  .242E+01
        9  .790E+19  .250E+01
       10  .505E+19  .225E+01
       11  .250E+19  .100E+01
     MESH NEUTRAL AND ION DENSITIES
    POINT (INCREASING CHARGE)
        1  .110E+01  .818E+02  .262E+03  .607E+06  .253E+10  .524E+13  .265E+17  .173E+18  .334E+18
        2  .287E+02  .816E+02  .262E+03  .607E+06  .253E+10  .783E+13  .324E+17  .180E+18  .329E+18
        3  .382E+04  .110E+05  .368E+05  .212E+08  .124E+11  .156E+14  .499E+17  .201E+18  .315E+18
        4  .496E+06  .145E+07  .554E+07  .109E+10  .194E+12  .504E+14  .856E+17  .226E+18  .285E+18
        5  .535E+08  .161E+09  .808E+09  .559E+11  .415E+13  .280E+15  .145E+18  .236E+18  .238E+18
        6  .605E+10  .198E+11  .103E+12  .253E+13  .818E+14  .197E+16  .228E+18  .216E+18  .181E+18
        7  .458E+12  .151E+13  .801E+13  .907E+14  .129E+16  .124E+17  .313E+18  .169E+18  .127E+18
        8  .231E+14  .790E+14  .353E+15  .221E+16  .139E+17  .538E+17  .350E+18  .116E+18  .839E+17
        9  .504E+15  .228E+16  .816E+16  .281E+17  .735E+17  .110E+18  .264E+18  .702E+17  .504E+17
       10  .459E+16  .251E+17  .613E+17  .874E+17  .665E+17  .546E+17  .123E+18  .331E+17  .236E+17
       11  .104E+17 0.         0.         0.         0.         0.         0.         0.
ENERGY LOSSES DUE TO IMPURITIES
     MESH          IONIZATION       RECOMBINATION          BREMS          EXCITATION
     POINT                                              STRAHLUNG
        1            .643E+05          .659E+04          .635E+03          .300E+05
        2            .662E+05          .652E+04          .620E+03          .319E+05
        3            .699E+05          .636E+04          .578E+03          .371E+05
        4            .707E+05          .582E+04          .508E+03          .440E+05
        5            .631E+05          .475E+04          .413E+03          .492E+05
        6            .474E+05          .325E+04          .305E+03          .480E+05
        7            .413E+05          .184E+04          .201E+03          .430E+05
        8            .751E+05          .112E+04          .113E+03          .725E+05
        9            .136E+06          .115E+04          .473E+02          .232E+06
       10            .586E+05          .622E+03          .100E+02          .274E+06
       11            .137E+04          0.                .296E+00          0.


***THIS CASE WAS PROCESSED BY TOPIC IN    5.54 SECONDS***
```